Solvation effects on association reactions in microclusters: Classical trajectory study of H+Cl(Ar)$_n$

Burkhard Schmidt[a] and R. Benny Gerber
Fritz Haber Research Center for Molecular Dynamics and Department of Physical Chemistry, The Hebrew University of Jerusalem, Jerusalem 91904, Israel, and Department of Chemistry, University of California, Irvine, California 92717

(Received 10 December 1993; accepted 18 March 1994)

The role of solvent effects in association reactions is studied in atom-cluster collisions. Classical trajectory studies of the systems H+Cl(Ar)$_n$ (n=1,12) are used to investigate the influence of size, structure, and internal energy of the "microsolvation" on the H+Cl association reaction. The following effects of solvating the chlorine in an Ar$_n$ cluster are found. (1) In the H+ClAr system there is a large "third body" effect. The single solvent atom stabilizes the newly formed HCl molecule by removing some of its excess energy. The cross section found at low energies is a substantial fraction of the gas-kinetic cross section. The molecule is produced in highly excited vibrational-rotational states. (2) Some production of long-lived HCl···Ar complexes, with lifetimes of 1 ps and larger, is found for the H+ClAr collisions. Weak coupling stemming from the geometry of the cluster is the cause for long life times. These resonance states decay into HCl+Ar. (3) At low collision energy (E=10 kJ/mol) for H+Cl(Ar)$_{12}$, the H+Cl association shows a sharp threshold effect with cluster temperature. For temperatures $T\geqslant$45 K the cluster is liquidlike, and the reaction probability is high. For $T\leqslant$40 K the cluster is solidlike, and there is no reactivity. This suggests the potential use of reactions as a signature for the meltinglike transition in clusters. (4) At high collision energies (E=100 kJ/mol) H atoms can penetrate also the solidlike Cl(Ar)$_{12}$ cluster. At this energy, the solid–liquid phase change is found not to increase the reaction probability.

I. INTRODUCTION

Association reactions of atoms and radicals to form stable molecules are among the most fundamental chemical processes.[1–3] Unlike the reverse process of dissociation[4] recombination of atoms and/or radicals to form stable molecules is far less well characterized. Both these types of processes are of fundamental importance, and were extensively studied in liquid solutions.[5] The solvent particles may affect the interaction potentials between the reagents, but typically more important are dynamical effects that occur in collisions between the reactive species or the products, and the molecules of the liquid. Most prominently, there is the "cage effect" which was first discovered by Franck and Rabinovitch in 1934.[6] They suggested that in photodissociation of iodine the fragments recoil from their solvent neighbors. These repeated collisions may hinder their separation which eventually leads to recombination. This process has an analog in the intimately related process of association. There the screening of atoms and radicals in a dense solvent can make it more difficult or even impossible for them to come into close contact and to recombine.

The prototypical example of I_2 has been a major testing ground for various experimental and theoretical methods to study photodissociation/geminate recombination processes. Besides photolysis experiments in liquids[7–9] and in gases[10–13] also trajectory calculations[14] and model calculations[15] have been employed to interpret the experiments. Another way of exploring solvent effects is to study photochemical processes, for instance, in the well-defined environment of rare gas matrices. Both experimental[16–20] and theoretical[21–23] work demonstrated the effects of the rare gas cage, including the role of its constrained geometry, on the dynamics of photo-induced reactions.

Besides the cage effect there is another important solvent effect in recombination reactions. For an association to occur the presence of at least one further atom or molecule is necessary. If this "third particle" removes sufficient energy to bring the molecule below dissociation threshold, it keeps the collision partners from dissociating again and thus leads to stabilization of the newly formed molecule. This is the well-known "third body" or "chaperon" effect.[1,24] A closely related question is the mechanism of energy relaxation in a solvent. Following an association the molecular product is initially very highly excited. By subsequent electronic, vibrational, and/or rotational energy transfer to the solvent it approaches thermal equilibrium with its environment.

It is obviously advantageous to explore the solvation effects on association reactions as mentioned above in a simple framework that permits detailed theoretical treatment. This makes an investigation of these processes in van der Waals or hydrogen bonded clusters especially promising. There has been great progress in cluster research both in physics and in chemistry trying to bridge the gap between gas phase and condensed matter behavior.[25–27] The enormous evolution of this field has been made possible by new experimental methods such as molecular beams and spectroscopic techniques. On the other hand the area also benefits substantially from the theoretical tractability of finite size aggregates. Stimulated by the availability of more and more powerful computers various classical and quantum mechanical simulation

[a]Present address: Freie Universität Berlin, Institut für Physikalische und Theoretische Chemie, Tabustr. 3, D-14195 Berlin, Germany.

 0021-9606/94/101(1)/343/13/$6.00

methods have been developed. Naturally, cluster studies are also emerging as an important tool in studies of chemical reaction dynamics and the role of solvation effects in these processes.

Many recent studies deal with solvation effects for a molecule embedded in a rare gas cluster. Information about structure and dynamics of this "microsolvation" is obtained from frequency shifts in vibrational[28] or electronic[29] spectroscopy where important size effects were first detected. Such systems were also used to study solvent effects on photoinduced reactions. Photolysis of dihalogens in rare gas clusters has been extensively studied, both experimentally[30–35] and theoretically.[36–38] These studies showed a strong dependence of the cage effect on the cluster size. Furthermore, it turned out that even one solvent atom may be sufficient to induce some caging. The photodissociaion dynamics of hydrogen halides was also the topic of considerable attention. Systems simulated were HI in $HI(Xe)_n$ ($n=1,5,12$) (Ref. 39) and HCl in $HCl(Ar)_n$ ($n=1,2$).[40–44] In these cases the existence of very light H atoms suggests the application of quantum mechanical simulation techniques. Using mixed quantum/classical or quantum/semiclassical schemes, quantum resonances and interference effects for the $Ar\cdots HCl \xrightarrow{h\nu} H+Cl+Ar$ photodissociation process were found.[43]

Most of the above-mentioned studies treat a recombination reaction as a reverse dissociation that occurs if caging prevents the mutual separation of fragments. It is, however, also interesting to study it as a bimolecular process occurring in collisions. Applying a crossed beam technique association reactions of O atoms with clusters of NO (Ref. 45) and CO (Ref. 46) were investigated demonstrating the "third body" effect. In another class of experiments reactive collisions of Ba atoms with N_2O clusters[47] and $N_2O(Ar)_n$ complexes[48] were observed. A closely related process, reactive collisions of O atoms with hydrocarbons bound in clusters was also studied.[49] On the theoretical side there have been classical trajectory simulations of recombination reactions in clusters. In extensive studies of $CH_3+H(Ar)_n$ ($n=4,12,13$) (Ref. 50) and of $I+I(Ar)_n$ ($n=12,54$) (Ref. 51) collisions relative roles of the chaperon effect, caging, and trapping of the reactants were explored.

The topic of the present work is the H+Cl recombination reaction in clusters. Solvation effects are illustrated here by attaching a varying number of Ar atoms to the chlorine reagent. Classical trajectory studies are carried out to simulate the $H+Cl(Ar)_n$ collision process. The computational methods employed here are described in Sec. II. The initial conditions are chosen to represent a crossed beam experiment. Analysis of final distributions allows the extraction of several experimentally relevant observables. These are partial cross sections for vibrational-rotational states of the HCl molecules and velocity and angular distributions for the HCl product.

To illustrate the strong size dependence of solvation effects in clusters two different extremes will be treated in the following. (1) In Sec. III we will present results for the case of a "single atom solvent." For the system H+ClAr the following questions will be addressed: How effective is the Ar atom stabilizing the HCl product ("third body" effect)? What is the partitioning of the product energy? What are the reaction mechanisms and how are they reflected in the translation of the products? What can we learn from the nonreactive scattering? (2) The case of a fully solvated Cl atom will be illustrated in Sec. IV. For the $H+Cl(Ar)_{12}$ system the following topics will be discussed: What is the cluster structure and what are possible reaction paths for a penetration of the Ar shell? What are the mechanisms of recombination and how effective is the vibrational/rotational relaxation of the HCl molecule? Temperature effects of the $Cl(Ar)_{12}$ complex and the question of the "melting transition" are studied in Sec. V. It will be of special interest how these phenomena are reflected in the reactivity of the H+Cl association, and, especially, whether there is a "signature" of melting. In Sec. VI our results are summarized and further developments of the theoretical models are discussed.

II. MODEL SYSTEM, METHOD, AND CALCULATION

A. Interaction potentials

The total interaction potential for the $H+Cl(Ar)_n$ collision system is constructed as a sum of pairwise interactions between the atoms. The four different atom–atom potential functions required for this system were taken from the literature. For the Ar–Ar interaction we choose the HFD-B2 model of Aziz and Slaman which was fitted to reproduce the best available spectroscopic, scattering, and bulk data.[52] The depth and position of the potential minimum are 1.19 kJ/mol and 376 pm, respectively. A model for the Ar–Cl interaction is taken from the analysis of atomic beam experiments carried out by Aquilanti *et al.*[53] Neglecting the weak anisotropy of the interaction between the rare gas atom and the open shell system $Cl(^2P)$ we only use the $V_{3/2,1/2}$ potential curve with a minimum of 1.46 kJ/mol at an interatomic separation of 378 pm. While the range is comparable for the two systems the deeper potential well is due to the higher polarizability of the Cl atom. The interaction of the Ar–H pair, however, is much weaker. The potential used here is the semiempirical model of Tang and Toennies predicting a shallow attractive well of only 0.45 kJ/mol located at a distance of 354 pm.[54] For the H–Cl interaction we use a Morse oscillator

$$V(r)=D_e\{1-\exp[-\beta(r-r_e)^2]\} \tag{1}$$

to represent the bound state $X\,^1\Sigma^+$ potential. Standard parameters of this potential function[55] are given in Table I.

Except for the H–Cl interaction all the other potential functions mentioned in the previous are represented by complicated analytical functions with up to 14 parameters (Ar–Cl). This makes simulations computationally very expensive, since in trajectory calculations most of the computer time is required for the calculation of forces. However, the numerical effort can be reduced substantially by fitting a simple analytical model to the potential functions. This is done here using a Buckingham model of the form[56]

$$V(r)=A\,\exp(-Br)-\frac{C}{r^6}\,. \tag{2}$$

TABLE I. Parameters of the pair potential functions for the H+Cl(Ar)$_n$ system.

	Buckingham potential parameters[a]		
	A (10^6 kJ mol^{-1})	B (10^{10} m^{-1})	C (10^{-60} kJ mol^{-1} m^6)
Ar–Ar	1.526	3.845	5563.
Ar–Cl	0.814	3.601	6987.
Ar–H	0.159	3.681	1475.
	Morse potential parameters[b]		
	D_e (kJ mol^{-1})	r_e (10^{-10} m)	β (10^{10} m^{-1})
H–Cl	445.5	1.275	1.868

[a]Parameters are obtaind by a least square fit of a Buckingham potential model given in Eq. (2) to each of the pair potential functions specified in the text.
[b]Parameters of the HCl ($X\,^1\Sigma^+$) Morse potential given in Eq. (1).

The resulting parameters of the values A, B, and C for each of the three pair interactions are listed in Table I.

A more realistic description of the system investigated here would also have to include three-body potentials. Especially for the Ar$_n$–HCl system there have been major efforts in this direction.[57–60] There are definitely discrepancies between the sophisticated Ar–HCl intermolecular potential functions derived by Hutson from high-resolution spectroscopic data[59(a)] and the pairwise potential used here for the H+ClAr system. We did not use the potential of Ref. 59(a), because it was calibrated from spectroscopic data for the $v=0$ and $v=1$ state of Ar$\cdots$HCl(v),[59(b)] which are sensitive to interatomic configurations completely different from those relevant for the processes studied here. Data on Ar$\cdots$HCl(v) for high v is, unfortunately, not available. For larger interatomic distances the pairwise potentials seem to be a reasonable approximation. It is, however, noted that it would be of great importance to study the influence of multibody interactions on chemical reaction dynamics in H+ClAr which we neglect here.

B. Classical cross sections

In this section standard techniques for the calculation of cross sections of bimolecular reactions from classical trajectories are briefly reviewed and applications to the systems studied here are discussed. In trajectory studies the probability P_Λ for any (reactive or nonreactive) process Λ can be simply evaluated as

$$P_\Lambda=\frac{N_\Lambda}{N}, \tag{3}$$

where N_Λ is the number of trajectories leading to the desired event Λ and N is the total number of trajectories. Consider atom–molecule collisions at a given collision energy $E_{\rm coll}$. Then the probability P_Λ in general is a function of (i) the (classical) impact parameter b of the collision; (ii) the orientation of the molecular partner which is specified here by the Euler angles Φ, Θ, Ψ;[61] and (iii) the internal degrees of freedom given by the classical variables v and J of vibration and rotation, respectively. Thus,

$$P_\Lambda(E_{\rm coll})=P_\Lambda(E_{\rm coll};b,\Phi,\Theta,\Psi;\mathbf{v},\mathbf{J}). \tag{4}$$

Partial cross sections for arbitrary processes Λ are then obtained by statistically averaging the trajectory computed probability P_Λ of this process[62]

$$\sigma_\Lambda(E_{\rm coll})=\int_0^\infty 2\pi b\,db\int_0^{2\pi}\frac{1}{2\pi}\,d\Phi\int_0^{\pi}\frac{1}{2}\sin\Theta\,d\Theta \times\int_0^{2\pi}\frac{1}{2\pi}\,d\Psi\int_0^\infty d\mathbf{v}\int_0^\infty d\mathbf{J}F(\mathbf{v},\mathbf{J}) \times P_\Lambda(E_{\rm coll};b,\Phi,\Theta,\Psi;\mathbf{v},\mathbf{J}), \tag{5}$$

where $F(\mathbf{v},\mathbf{J})$ is a distribution function corresponding to the vibration and rotation of the molecule (see below). Note that for the case of a diatom the orientation can be described by two polar angles Θ and Ψ only and the integration over Φ can be omitted.

The numerical evaluation of the multidimensional integrals of the form of Eq. (5) is routinely done by an approximative Monte Carlo procedure. This technique has the advantage of being independent of the dimensionality of the problem. This, however, goes at the price of a slow convergence. The Monte Carlo error only decreases as $n^{-1/2}$ with n being the number of integration points. Therefore, the number of trajectories in the simulations presented here has to be relatively high. In order to keep the error of the partial cross sections well below 10%, typically about 10^5 trajectories have to be evaluated.

C. Details of the trajectory calculations

1. Initial conditions

For each integration point of the Monte Carlo procedure one trajectory has to be run. Initial conditions are selected according to all the integration variables. All calculations are done in the center of mass system and the colliding partners are assigned a relative velocity corresponding to $E_{\rm coll}$. The vector of initial separation $\boldsymbol{\rho}$ has to be chosen so that the particles are outside the range of their mutual interaction. Typical values for ρ are $\rho=1$ nm for the H+ClAr case and $\rho=1.5$ nm for the H+Cl(Ar)$_{12}$ system. The component of $\boldsymbol{\rho}$ perpendicular to the relative velocity is given by the impact parameter b. The integration over this variable is extended up to a maximum parameter b_M, where the reaction probability P_Λ practically vanishes. Convergence tests show that values of $b_M=1$ nm and $b_M=2$ nm are sufficient for the two systems, respectively. The initial orientation of the Cl(Ar)$_n$ complex is achieved by rotations with a Euler matrix corresponding to the angles Φ,Θ,Ψ.[61] The remaining variables $\mathbf{v}$ and $\mathbf{J}$ represent the internal degrees of freedom of the molecular collision partner. For reasons of simplicity, our vibrational-rotational treatment of the H+ClAr system corresponds to a simple classical limit of the $v=0$, $J=0$ quantum initial state of the dimer. The interatomic distance of the ClAr dimer is kept frozen at the equilibrium value and rota-

tional motion of the diatom is neglected. However, the calculations include sampling of all possible initial orientations of the ClAr diatomic "molecule" with respect to the incoming H atom. Physically, we expect indeed the orientation (rather than the vibration) to be the parameter determining reactivity in this system. In the investigation of the $H+Cl(Ar)_{12}$ system we obtain $F(\mathbf{v},\mathbf{J})$ by sampling from a microcanonical ensemble. This enables us to study thermal effects in the $Cl(Ar)_{12}$ complex. For more details of this procedure, see Sec. V.

2. Integration of the equations of motion

Starting with the initial conditions specified in the previous, Newton's equations of motion have to be solved. This is done numerically using a Gear predictor–corrector scheme of sixth order.[63] A special problem encountered in the recombination processes are the different orders of magnitude of the interatomic forces. It is advisable to employ a relatively large time step for the time where the evolution of the trajectories is governed by the weak van der Waals forces. Once the much stronger chemical forces between the H and the Cl atom become effective the time step has to be reduced substantially. Therefore, we scale the step size with the maximum component of the accelerations. Typically in a reactive trajectory for $E_{coll}=10$ kJ/mol the time step varies from 10 fs down to 0.1 fs.

3. Final conditions

Each trajectory is run until either one of two conditions is met. (1) If no reaction occurs the distance of the collision partners has to reach the value of the initial separation ρ (asymptotic distance), or (2) if an HCl molecule was formed the distance between the moiety and each of the Ar atoms has reached a value at least as large as ρ. In the latter case some observables of the newly formed molecule are of interest. First of all, the internal energies of vibration (E_{vib}) and rotation (E_{rot}) are calculated. Treating vibration-rotation coupling only to first approximation the quantized energy levels of a diatom can be expressed as

$$\frac{E_{vib}(v)}{hc}=\omega_0(v+\tfrac{1}{2})-\omega_0\chi(v+\tfrac{1}{2})^2 \tag{6}$$

and

$$\frac{E_{rot}(J)}{hc}=BJ(J+1)-D[J(J+1)]^2. \tag{7}$$

The constants are obtained within the "rotating Morse oscillator" approximation using the parameters for the HCl molecule as given in Table I. The harmonic frequency ω_0 and the anharmonicity $\omega_0\chi$ are 3002 and 60 cm^{-1}, respectively, the rotational constant is $B=10.7$ cm^{-1} and the centrifugal distortion is $D=0.000\,54$ cm^{-1}. Approximate quantum numbers of vibration and rotation are then calculated by inverting Eqs. (6) and (7) and rounding the values to the nearest integer numbers. This allows one to obtain partial cross sections for individual internal states (v,J) of the HCl product.

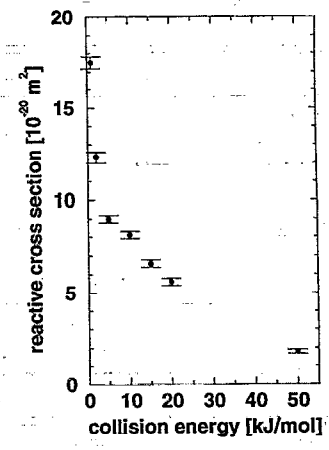

FIG. 1. Energy dependence of the total reactive cross section of the H+ClAr→HCl+Ar association reaction.

III. ONE ATOM ACTING AS A SOLVENT: H+ClAr

A. Third body effect

In a first series of simulations the H+ClAr→HCl+Ar reaction is studied. Special emphasis will be on the solvent effect which is modeled here by attaching a single Ar atom to the Cl reagent. We want to investigate the third body effect induced by this atom on the reactivity of the HCl recombination. Total reactive cross sections for the H+Cl association are obtained by calculating the probability P_Λ [see Eq. (3)] of a trajectory leading to formation of an HCl molecule and statistically averaging according to Eq. (5). In this way cross sections are evaluated for different collision energies. The reactive cross sections σ_R shown in Fig. 1 decrease monotonically from 17.5×10^{-20} m^2 for $E_{coll}=1$ kJ/mol down to less than 2×10^{-20} m^2 for $E_{coll}=50$ kJ/mol. That means that for a typical experimental energy of a hydrogen atom beam of about 10 kJ/mol the cross section is in the order of 10^{-19} m^2 and still well above the sensitivity threshold of state-of-the-art experiments.

The steep falloff of these cross sections with increasing collision energy can be quantitatively understood in the following way: Because the potential surface for the recombination reaction has no barrier the only mechanisms limiting the reactivity must be of dynamical nature. Assuming the centrifugal force alone to provide the barrier for the reaction it can be shown that in the framework of a Langevin model the cross section decreases according to a power law, $(E_{coll})^{-2/s}$, where $(-s)$ is the power of the long range part of the potential.[64] This dependence of the reactivity on the collision energy is found here qualitatively, but quantitatively there are discrepancies caused by the more complicated reaction mechanisms. Another striking feature is that, although large enough to be measured, the reactive cross sections are relatively small compared to the long range of the strongly attractive H–Cl interaction. This reflects the inefficient coupling of the HCl and the ClAr modes of motion. Aside from the weakness of the coupling induced by the H–Ar potential there is another and more important reason for this which is the separation of mass-scale between H and the other two

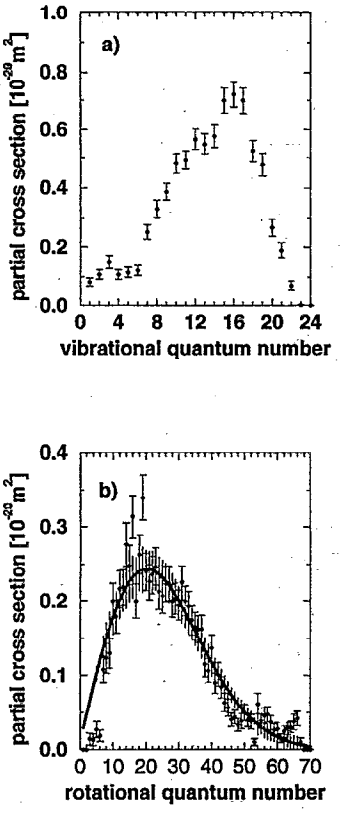

FIG. 2. Partial cross sections of the H+ClAr→HCl(v,J)+Ar reaction at a collision energy of 10 kJ/mol. (a) Distribution of the vibrational states of the HCl product. (b) Distribution of the rotational states.

atoms. Rearrangement reactions of atoms for such mass scales are relatively inefficient.[65] Using a D atom instead of an H atom does not change the ratio of the masses sufficiently. For a collision energy of 10 kJ/mol the cross section increases only by 20% upon deuteration. The reactivity is, however, expected to be substantially higher for recombinations of dihalogens like the Cl+ClAr system.

B. Partitioning of the energy release

The HCl association reaction is a highly exothermic process. Assuming a collision energy of 10 kJ/mol the exothermicity of the reaction is given by

$$\Delta E=\Delta E(\mathrm{HCl})-\Delta E(\mathrm{ClAr})+E_{\mathrm{coll}}$$
$$=(445.5-1.4+10)\ \mathrm{kJ/mol}=454.1\ \mathrm{kJ/mol}. \quad (8)$$

Upon combination of the two reactants and separation of the Ar atom there are three different channels of product energy. Vibration and rotation of the HCl diatom and the relative translation of HCl vs Ar. In order to quantify the specificity of this energy release we calculate partial cross sections for the individual product states of the HCl molecule, within our "box quantization" treatment of the classical results.

The upper panel of Fig. 2 shows the population of vibrational states. The distribution is very broad and highly inverted with its maximum at a quantum number $v=16$ corresponding to a vibrational energy of 395.5 kJ/mol. Towards higher quantum number this distribution stretches to the third highest oscillator level $v=22$. On the other hand there are also trajectories where the HCl molecule is cooled down to the $v=1$ state. In the lower part of the figure we see the distribution of the rotational states. In accord with the result for the vibration this also indicates an extremely high excitation of the molecule. The maximum of the curve is found at $J=20$ or at a rotational energy of 53.6 kJ/mol. With the exception of the first few points this distribution can be fit very well by a Boltzmann-type curve. The resulting temperature is higher than 13 000 K.

Assuming a trajectory with product states corresponding to the maxima at $v=16$ and $J=20$ the following picture for the energy partitioning emerges. As much as 87% of the released energy is channeled into vibrational motion while 12% of the product energy appears as rotation of the HCl molecule. Hence, the high excitation of the diatom leaves only about 1% of the available energy (or 5 kJ/mol) in the translation of the products. This strongly nonstatistical result will be elucidated further in the following. If HCl were formed at low excitations, this would correspond to a "multiquantum" relaxation of HCl by Ar, which is known to be inefficient also classically.

C. Product translation

To obtain a more complete picture of the energy release and to gain understanding of the reaction mechanisms it is instructive to consider the distributions of velocity and scattering angle of the HCl product. Furthermore, these quantities are accessible in a differential scattering experiment. Again we restrict ourselves to the case of a relative collision energy of 10 kJ/mol. The velocity distribution of the HCl molecule can be seen in the top half of Fig. 3. Its structure is clearly bimodal with two maxima at $v\approx0.2$ km/s and at $v\approx0.7$ km/s. Because all calculations are carried out in the center of mass system conservation of momentum allows us to obtain the corresponding Ar velocity and thus the total translational energy of the two products HCl and Ar. The values for the two maxima are 1.4 and 16.8 kJ/mol, respectively. There is a relatively sharp upper bound of the distribution at $v\approx0.8$ km/s. This gives us an estimate of the maximum translational energy of 22 kJ/mol or 5% of the available exothermicity. From this we can deduce that there must be strong correlation between vibrational and rotational energy. Although their distributions cover a range of about 400 and 100 kJ/mol, respectively, in total they always account for at least 95% of the available energy of the reaction.

The bottom half of Fig. 3 shows the angular distribution of the the HCl products. Although being very broad two regions of higher probability can be distinguished. With the scattering angle defined as 0° for the direction of the incoming H atom there is a main maximum in the region of forward scattering (180°) accompanied by a smaller maximum for backward scattering (0°). A closer inspection of the trajectory data reveals that there is a strong correlation between these two distribution. The backward scattered products are found to be faster ($v\approx0.7$ km/s) than the forward scattered ones ($v\approx0.2$ km/s).

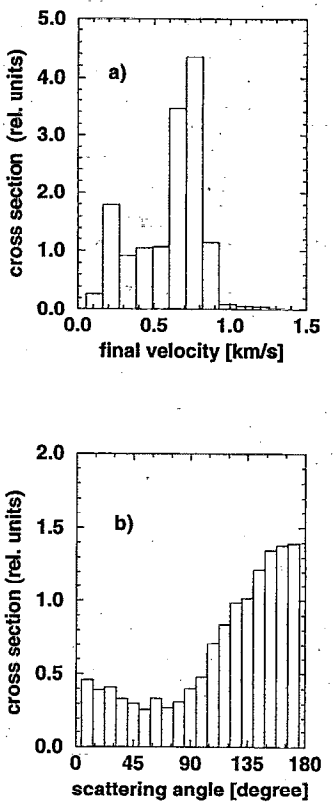

FIG. 3. Velocity and angular distribution (center of mass system) of HCl molecules formed in H+ClAr→HCl+Ar reactions at a collision energy of 10 kJ/mol. (a) Distribution of the HCl velocities. (b) Angular distribution of the HCl products. Note that a scattering angle of 0° corresponds to the direction of the incoming H atom (backward scattering).

D. Reaction mechanisms

The results given in the previous clearly suggest the existence of two different reaction mechanisms for the HCl formation. This is further investigated by studying the dependence of the recombination reaction on the initial orientation of the ClAr dimer. For illustration we show two prototypical examples of two-dimensional trajectories for $E_{coll}=10$ kJ/mol in Fig. 4. In the first case (a) the initial orientation is such that the Cl atom points towards the direction of the collision partner, in the second case (b) there is an angle of 135° between these two directions. In either case the reaction can be characterized by the same four steps. (1) The incoming H atom is captured by the strong attraction of the Cl atom leading to an orbit type of motion. In the course of this spiral the H–Cl distance is slightly decreasing which leads to an acceleration of the H atom. (2) The H atom then collides with the Ar atom. In this collision it transfers some fraction of its energy to the solvent atom causing the weak Ar–Cl bond to break. The H atom, which lost part of its kinetic energy, remains trapped in the attractive field of the Cl atom. (3) Then the newly formed molecule slowly leaves the reaction zone. The curled motion of the H atom is an indicator of the high vibrational and rotational excitation of the diatom. (4) Because of the slow separation of the products it is possible that the H atom in its wide amplitude motion undergoes further collisions with the Ar atom. One such impact can be seen in Fig. 4(a). Although these may be "soft collisions" they may further increase the energy associated with the relative translation of the HCl molecule vs the Ar atom.

It is interesting to consider the energy transfer in H–Ar collisions quantitatively. Dictated by the mass ratio of 1:40 a hydrogen atom cannot transfer more than 10% of its kinetic energy to the translation of the Ar atom. Therefore, the attractive interaction with the Cl atom before the H–Ar collision plays an important role. By accelerating the H atom which has an initial energy of only 10 kJ/mol it gains additional kinetic energy. Consequently, it is able to transfer even in a single collision an amount of several kJ/mol which is in agreement with the values of the kinetic energy found in the product translation (see above).

The only essential difference between the two example trajectories of Fig. 4 is that the HCl product is scattered into the backward (case a) and into the forward (case b) hemisphere. Further test calculations show that the direction of the separation of the products is essentially given by the initial orientation of the ClAr reactant. In other words, the forward scattered products are generated from H+ArCl approaches while the backward scattered HCl molecules are formed in collisions of the H+ClAr type. This behavior is again caused by the ratios of masses which makes a reorientation of the heavier atoms impossible.

As discussed previously, only a small fraction of the energy available is converted to relative translational motion of the products. This, and the relatively high masses of the Ar and HCl formed imply that the reaction process is not very

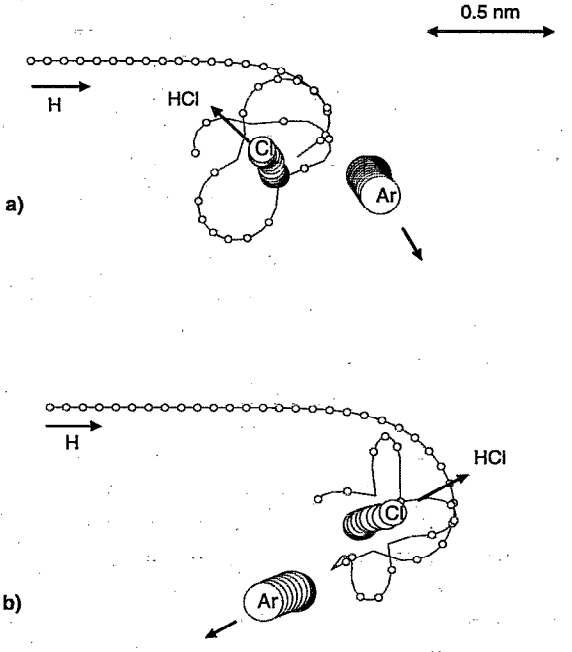

FIG. 4. Reaction mechanism of the H+ClAr→HCl+Ar reaction at an impact energy of 10 kJ/mol. The two examples of reactive trajectories represent different initial orientation of the ClAr dimer leading to recombination where the HCl product is scattered backwards (a) and forwards (b). The circles depict the positions of the three atoms at time intervals of 5 fs.

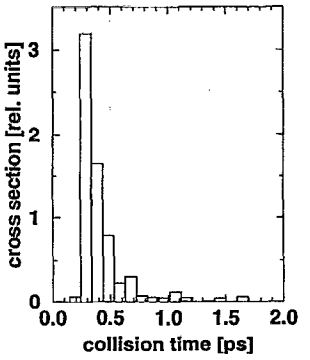

FIG. 5. Distribution of collision times of the H+ClAr→HCl+Ar reaction at a collision energy of 10 kJ/mol. Note that besides the maximum at $t\approx200$–700 fs there is some probability for the occurrence of long lived complexes ($t\sim1$–1.5 ps).

fast. Typically a reaction takes up to a few periods of vibration/rotation of the HCl until the mutual interaction of the products vanishes. This is illustrated in Fig. 5. The distribution of collision times for the H+ClAr reaction at an impact energy of 10 kJ/mol has a clear maximum in the region of 200–700 fs which corresponds to trajectories of the type shown in Fig. 4. In addition to that also some probability for very long collision times is found. This is caused by the occurrence of very long-lived HClAr complexes. In our trajectory calculations we found lifetimes of up to 10 ps. A more detailed analysis of these resonances shows how they are related to the initial geometry of the collision. They can only occur if (1) the ClAr axis and the direction of the initial H atom velocity form an angle of about 90° and if (2) at the same time the impact parameter is such that the height of the centrifugal barrier matches the initial energy. In these cases a metastable complex can be formed where the H atom rotates in a plane perpendicular to the ClAr axis. In this geometry, the coupling between the vibrational and rotational modes of the HCl and the motion of the Ar is very weak resulting in slow decay. An experimental search for these long-lived resonances, if feasable, should be of considerable interest.

IV. THE FIRST SOLVATION SHELL: H+Cl(Ar)$_{12}$

A. Cluster structure and potentials

The second system studied here is a fully solvated Cl reactant. In analogy to a pure Ar cluster it takes 12 atoms to build up a complete shell around the central atom. They arrange in an icosahedral symmetry (I_h) which was proposed many years ago.[66,67] Furthermore, icosahedral structures have indeed been observed in electron diffraction experiments with small Ar clusters.[68] This structure also represents a minimum energy configuration for the doped cluster with the chlorine situated in the center. Using the pair potentials of Sec. II A a total interaction energy of 53.9 kJ/mol is obtained.[69]

The interaction between the Cl(Ar)$_{12}$ complex and a H atom is highly anisotropic. Figure 6 shows potential energy curves for the three principal directions. (1) For an approach of an H atom along one of the C_5 axes towards a corner atom there is a steep repulsive wall at a center of mass separation of about 0.6 nm. (2) Along one of the C_2 axes intersecting each of the edges of the icosahedron a H atom can in principle penetrate the cage. There is a potential barrier of 160 kJ/mol that has to be overcome before the H atom is subject to the strong H–Cl attraction in the interior of the cluster. (3) The barrier height is reduced down to 58 kJ/mol for a penetration along one of the C_3 axes going through the center of each of the triangular faces of the icosahedron. Therefore the chance for recombination is highest for this direction. A typical value of the size of the "windows" of this cage is 10^{-20} m^2 for an impact energy of 100 kJ/mol. For this energy cage penetration is possible for approximately 13% of the surface of the icosahedral cluster. Note that the values for the penetration barriers and cage openings given here are obtained assuming the solvation shell to be rigid. This however, is a reasonable approximation. Because of the high velocity of the H atom and the inefficient momentum transfer to the heavy atoms the cluster is practically "frozen" on the time scale of the collision process.

Besides the strong repulsion of a H atom by a Cl(Ar)$_{12}$ complex there is also a weak van der Waals attraction between the two particles. As can be seen from the insert of Fig. 6 the corresponding well depth lies between 0.6 kJ/mol (C_5) and 1.7 kJ/mol (C_3). This suggests two different types of reactive events which are relevant for different regimes of the collision energy. (1) Recombination of H+Cl can occur only at energies high enough to overcome the barrier of at least 58 kJ/mol for cage penetration. (2) Capture of H atoms in the well of the dispersion forces is expected to be effective only at energies not much larger than the well depth. If such trapping happens it may be interesting whether there is a very slow process involving some restucturing of the cluster,

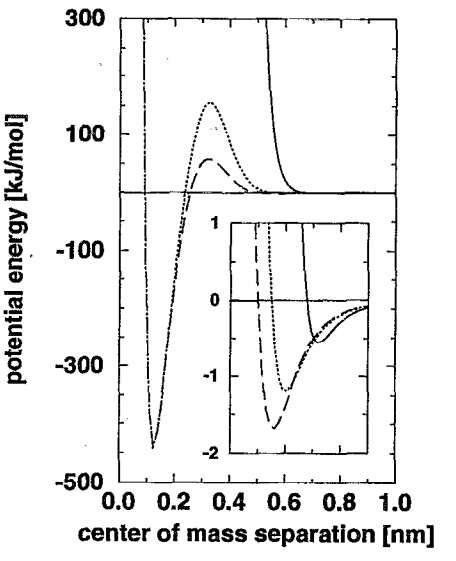

FIG. 6. Interaction potentials between a H atom and the Cl(Ar)$_{12}$ cluster along the three types of symmetry axes. Solid, corner (C_5); dotted, edge (C_2); dashed, face (C_3). The insert shows the region of the van der Waals attraction at an enlarged scale.

which leads to opening of the "windows" in the potential separating the H and the Cl. We shall now examine whether these processes are indeed realized.

B. Reaction mechanisms

A typical scenario of a trajectory leading to a recombination reaction is the following: (1) A H atom with a kinetic energy of 100 kJ/mol penetrates one of the triangular faces of the cluster. The direction of impact is parallel to one of the C_3 axes with an impact parameter of 50–100 pm. (2) Once inside the cage it is captured by the Cl atom in the center and begins an oscillatory wide-amplitude motion inside the solvation shell. (3) During the course of this part of the trajectory the H atom collides with the Ar atoms from inside the cluster. In these collisions the Ar atoms are boiled off from the cluster which finally leads to its complete decomposition. Typically, the dissociated atoms have kinetic energies in the range from 0.2 to 20 kJ/mol. As a consequence of this energy transfer the newly formed HCl molecule is stabilized and cooled down. This process of vibrational/rotational relaxation can be characterized by the time scale of the complete evaporation of the Ar shell, which is in the order of 1.5 ps. This is equivalent to an average interval of 100 fs between the subsequent ejection of two solvent atoms.

Although recombination events like this are possible, and in a directed search for optimal initial conditions we were able to generate a few examples, this process is of extremely low probability. In a typical Monte Carlo averaging over 10^4 trajectories there is not a single reactive event for an impact energy of 100 kJ/mol. All trajectories show almost elastic scattering of the H atom from the cluster surface. The situation is the same for other energies, too. In test calculation up to 1000 kJ/mol there are no reactive trajectories. This means that despite the appreciable size of the cage openings for these energies they do not contribute to the reactivity of the HCl recombination. The reason for this is that cage penetration is only possible in close collisions of the H atom. It can be seen from Eq. (4), however, that collisions at small impact parameters are of very low statistical weight. In addition, there are strong steric constraints. Therefore, the reactive cross section is zero for all practical purposes. It has to be noted that these results were obtained by setting the initial configuration of the $Cl(Ar)_{12}$ cluster to its icosahedral minimum energy structure for each trajectory. This is equivalent to assuming a cluster temperature of $T=0$ and ignoring zero-point motions. The effect of thermal motion of the atoms in the cluster will be subject of Sec. V where thermal effects on the reactivity will be studied.

It is interesting to compare our results with those of Hu and Martens.[51(a),51(b)] In classical trajectory studies of $I+I(Ar)_{12}$ collisions they found no cage effect. At a comparable energy of 104.6 kJ/mol they find a large reactive cross section for the I+I geminate association of 36.6×10^{-20} m^2 which increases strongly for lower impact energies. The remarkable discrepancy has two different reasons. First, the I–Ar interaction with a well depth of 1.56 kJ/mol is much stronger than the the H–Ar interaction. This leads to an increased capture rate for the iodine system. Second, after the capture the two reaction partners migrate to find each other and eventually association takes place. The relatively large energy release when the I atom is trapped destroys the rigidity of the cluster system, even if the latter was initially at $T=0$! In essence, for I colliding with $I(Ar)_{12}$ there is always sufficient energy to "crash" the cage. For this process the authors of the mentioned study give a probability of close to 100%. A similar observation was made by Del Mistro and Stace in trajectory calculations. A CH_3CN molecule positioned on the surface of an initially cold Ar_{20} cluster causes the cluster to melt, and then the molecule becomes solvated.[70] However, there is no analogon to melting and/or diffusion for the systems studied here.

To confirm this we perform further trajectory calculations at a collision energy of only 0.1 kJ/mol. In this low energy regime there is a high capture probability for the H atom, the resulting cross section for trapping of the projectile atom is found to be $(299\pm6)\times10^{-20}$ m^2, which is approximately two times the geometrical cross section. The physisorbed H atoms are initially able to move on the cluster surface. After a certain time, however, they have lost some fraction of their energy and they finally get trapped in one of the pockets of the van der Waals potential at one of the C_3 axes. Calculations of a few very long trajectories show that the trapped state is relatively long-lived. Evaporation of the physisorbed H atom from the cluster surface typically occurrs at a time scale of 100 ps to 1 ns. On this time scale there is no diffusion into the interior of the cage. Classically, the probability of association triggered by the energy deposited in the cluster by trapping of the H atom is at most an extremly rare event, and practically of zero weight. This leaves open the possibility of enhancement of the reactivity by quantum mechanical tunneling of the trapped H, an effect not included in our classical treatment. In conclusion, the probability for H+Cl association in collisions of H with $Cl(Ar)_{12}$ at $T=0$ is practically zero, at least in the classical framework.

V. TEMPERATURE EFFECTS

A. Preparation of the doped Ar clusters

In order to study thermal effects of the $Cl(Ar)_{12}$ cluster a series of molecular dynamics (MD) simulations for different temperatures is carried out. Based on the same pair potential approach as described above, Newton's equations of motion are solved using the same algorithm[63] as for the collisional problem with a constant time step of 10 fs. A simple way to perform simulations at a well defined temperature is sketched in the following.

(1) Scaling of the velocities: Over a period of 100 ps the velocities of the $N=13$ particles are scaled to reach the kinetic energy $E_{\rm kin}$ which is related to the desired temperature T by

$$T=\frac{2}{3N-6}\frac{E_{\rm kin}}{k_B}, \tag{9}$$

where k_B is Boltzmann's constant. This process of scaling is done in intervals of 5 ps (500 integration steps) and the velocities are not allowed to change by more than 10% each time. (2) Thermalization: To allow the system after this heat-

ing or cooling to reach thermal equilibrium the trajectory is continued for another 50 ps. (3) Statistical averaging: After the equilibration of the system is confirmed the third phase of the MD simulation begins. Over a long period of 10 ns (10^6 time steps) various observables are sampled at intervals of 20 ps for averaging. Among these quantities are the total and the kinetic energy as well as structural and dynamic properties which are discussed in the following chapter. This procedure is started at a temperature of 2 K and then iterated for a temperature increment of 2 K. Each time the final cluster configuration is used to initialize the next run. Note that although this method results in a sufficiently well defined temperature, the calculations of the trajectories are, of course, microcanonical in this approach, i.e., total energy rather than temperature is conserved.

At increasing temperature occasional evaporation of one of the atoms is found in our calculations. Therefore the length of the trajectories after equilibration has to be reduced to 1 ns for $T \geqslant 42$ K. Finally the simulations could not be pursued further for $T > 46$ K because of more frequent evaporation of atoms from the cluster.

B. Thermal and structural properties of the doped Ar cluster

As a very general feature of the thermal behavior of the $Cl(Ar)_{12}$ aggregate the caloric curve is considered first. It is obtained as the functional dependence of the cluster temperature calculated using relation (9) on the mean total energy. As shown in Fig. 7(a) this is a linear function up to a temperature of 36 K. At larger temperatures, however, there is a flattening of this curve which is associated by a sudden increase in the fluctuations. In order to get more detailed information about this transition we calculate the relative root mean square (rms) fluctuation δ of the bond length r_{ij} of any pair i and j of the N atoms in the cluster as

$$\delta = \frac{2}{N(N-1)} \sum_{i \neq j} \frac{(\langle r_{ij}^2 \rangle - \langle r_{ij} \rangle^2)^{1/2}}{\langle r_{ij} \rangle}, \tag{10}$$

where $\langle \cdots \rangle$ symbolizes trajectory averages. This number δ is often used as an indicator of the mobility of the atoms in a cluster. For condensed matter, according to the empirical Lindemann criterion, solid and liquid state are characterized by $\delta < 0.1$ and $\delta > 0.1$, respectively.[71] The temperature dependence of this quantity is shown in Fig. 7(b). After a slow linear increase up to $\delta = 0.06$ at $T = 36$ K reflecting the thermal expansion of the system there is a sudden rise of this number up to $\delta = 0.32$ at $T = 46$ K.

To characterize the nature of this transition more in detail we animate the trajectory with the help of computer graphics. A series of snapshots is shown in Fig. 8. At a temperature of 40 K the dynamics of the $Cl(Ar)_{12}$ cluster is governed by large amplitude vibrational motions. As illustrated in Fig. 8(a) there can be substantially stretched bonds between neighboring Ar atoms which cause craterlike openings in the solvation shell. However, the basic icosahedral structure remains intact and there is no free mobility of the atoms. Despite the large bond length fluctuations of $\delta = 0.23$ the cluster is still solidlike at this temperature. At a temperature of 45 K this value rises further to $\delta = 0.31$ and now the picture completely changes. New types of cluster configurations are accessible as can be seen in Fig. 8(b). (1) Ar atoms may occupy sites in the second shell thereby leaving holes in the first solvation shell. (2) On longer time scales there can be complete rearrangements of the atoms, as well. The chlorine can migrate to the surface of the aggregate, and there is no resemblance with the initial icosahedral symmetry anymore. These irregular fluctuating structures combined with an increased freedom of the particle motion indicate the presence of a liquid phase at this temperature.

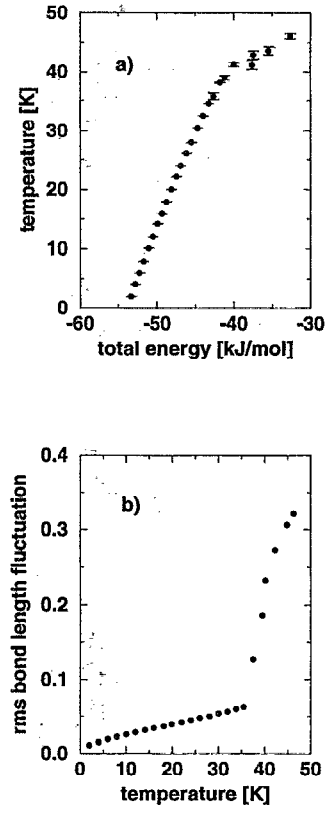

FIG. 7. Thermal and structural properties from MD simulations of the $Cl(Ar)_{12}$ aggregate. (a) Caloric curve. (b) Relative rms fluctuation of the bond lengths as defined in Eq. (10).

We conclude that there must be a solid–liquid-like phase change in the region between $T = 40$ and 45 K. Analogous observations were made previously for the pure Ar_{13} cluster where a transition was found at a temperature of 34 K.[72,73] The lower temperature of this transition is due to the weaker Ar–Ar interaction model assuming a well depth of only 1.006 kJ/mol and due to the absence of the slightly stronger interaction with the chlorine atom. The question of a coexistence region with spontaneous transitions between rigid and nonrigid behavior and vice versa cannot be answered here because of the less extensive data. However, we found no such jumps even in long MD runs of 1–10 ns for the $Cl(Ar)_{12}$ system at $T = 40$ and 45 K.

C. Temperature dependence of reactivity

In the following we study the reactivity of H+Cl recombination in $H+Cl(Ar)_{12}$ collisions as a function of the inter-

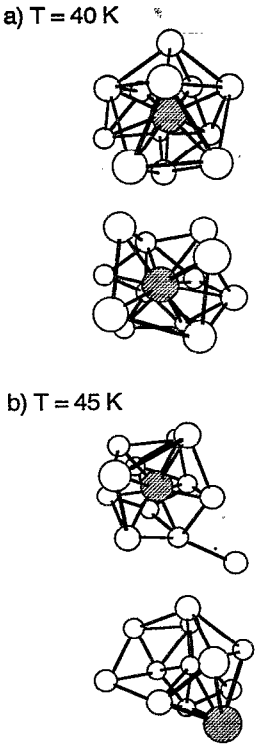

FIG. 8. Snapshots of configurations of the $Cl(Ar)_{12}$ cluster obtained from the MD simulations. (a) At $T=40$ K the cluster is still solidlike. (b) At $T=45$ K the cluster is in a liquidlike phase. The filled circle represents the Cl atom.

nal energy of the solvent cluster. This means that the probabilty P_Λ computed from the trajectories must be integrated over the internal degrees of freedom as indicated by $\int d\mathbf{v}\int d\mathbf{J}F(\mathbf{v},\mathbf{J})$ in Eq. (5). In our computer simulations this is done by sampling and storing 200 different configurations together with velocities and higher derivatives required for the Gear sixth order algorithm from the thermal MD simulations of the cluster. They are then used to initialize the trajectories of the atom-cluster scattering calculations.

Figure 9 shows the temperature dependence of the total reactive cross section for two different collision energies and for a selection of different cluster temperatures. The first series of simulations is carried out for a collision energy of 10 kJ/mol. This energy is far below the barrier for penetration of a H atom assuming the cage formed by the 12 Ar atoms to be rigid (see Sec. IV A and Fig. 6). Accordingly, we see no reactions up to a temperature of $T=20$ K. The data points for $T=30$, 35, and 40 K indicate that for these temperatures there is some very small probability for recombination reactions. However, even at $T=40$ K where the vibrations of the atoms are already of large amplitude as shown in Fig. 8(a) and as characterized by the large value of $\delta=0.23$ the reactive cross section remains below 0.5×10^{-20} m^2. This changes drastically above the transition temperature of the $Cl(Ar)_{12}$ aggregate. The cross section rises up to 11.4×10^{-20} m^2 at $T=45$ K. This can be explained in a straightforward manner. Due to the free mobility of the atoms in the liquidlike regime there is a certain chance to find the Cl at the surface which accounts for most part of the sudden increase in reactivity of the H+Cl recombination. Likewise, the H atom can penetrate into the cluster with significant probability when the cluster is liquidlike.

The role of thermal effects on the reactivity is distinctly different at higher impact energies. The total reactive cross section for atom-cluster collisions with an energy of 100 kJ/mol can be seen in Fig. 9(b). As already discussed in Sec. IV B there is no reactivity for the case of a rigid cluster ($T=0$) although the H atoms are in principle fast enough to overcome the barrier for cage penetration. This, however, changes when we allow thermal motion of the atoms in the cluster. Already at $T=10$ K we find a cross section of 0.5×10^{-20} m^2 which increases up to $(1.5–2)\times10^{-20}$ m^2 at 40 K. For cluster temperatures above the solid–liquid phase change, a slightly lower total cross section for the HCl association reaction is found. Given the relatively large uncertainties of the Monte Carlo integration it can be said that the reactivity is essentially unchanged upon transition to the liquid phase of the cluster.

A qualitative explanation for this is a steric effect in collisions with clusters bearing the chlorine atom on an outer corner. For H atoms attacking from the right side the enhanced exposure of the Cl atom clearly contributes to the reactivity. For H atoms approaching from the other side the two reactants are shielded by a cluster of 12 Ar atoms which is very unlikely to be penetrated. It is the tradeoff between these two effects which keeps the reactivity from increasing upon solid–liquid phase change like for low impact energies. As can be seen from the large cross section for the $E_{coll}=10$ kJ/mol collisions for the liquidlike cluster at $T=45$ K the

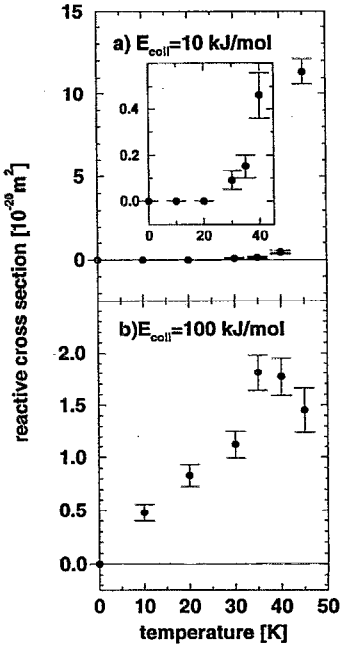

FIG. 9. Temperature dependence of the total reactive cross section for $H+Cl(Ar)_{12}\rightarrow HCl+12Ar$ recombination processes for two different relative energies of the reactants. (a) $E_{coll}=10$ kJ/mol. (b) $E_{coll}=100$ kJ/mol.

same argument does not apply there. In that case H atoms approaching from the opposite side of the Cl can be deflected to surround the cluster in a similar manner as illustrated in Fig. 4(b) for the atom–diatom system. This also explains why this cross section is even 46% larger than the corresponding value for the H+ClAr system. The capture of the H atoms by the long range atom–cluster interaction enhances the reactivity of the $H+Cl(Ar)_{12}$ system. In any case, the dramatic difference between solidlike and liquidlike states of the cluster with respect to recombination for collisions at low energies suggests an exciting possibility of using chemical reactions as an experimental signature for the state, or type of phase of the cluster. If the temperature of the cluster can be controlled, perhaps the melting transition can be observed since the effect is so sensitive.

VI. SUMMARY

In this article the role of microscopic solvation on the dynamics of association reactions is studied theoretically. In classical trajectory studies of atom-cluster collisions for the model system $H+Cl(Ar)_n$ we illustrate the effects of solvating one of the reactants by a rare gas van der Waals cluster. For these prototype systems we illustrate how size, structure, and internal energy of the $(Ar)_n$ microcluster affect the reactivity of the HCl recombination. In order to make our results comparable to future experiments the initial conditions of the trajectories are chosen to resemble a crossed beam scattering experiment. Partial cross sections for individual internal states of the HCl molecule as well as velocity and angular distributions of the products are obtained in these calculations.

One fundamental solvent effect is the "third body" or "chaperon" effect which is studied here for the case of a single solvent atom. In H+ClAr collisions permanent association of the two radicals can only occur if the incoming H atom undergoes a collision with the Ar atom immediately after being captured by the Cl atom. In this way some energy is removed from the newly formed HCl molecule which is thereby kept from redissociating. For this reason the energy transfer associated with the H–Ar collisions plays a crucial role for the recombination. The dynamics of this collision governs the reaction mechanism in the following ways. First of all, through the implications of mass-scale seperation between H and Ar,Cl they limit the overall reactivity. Despite the strong H–Cl attraction and the lack of barriers on the potential surface the total reactive cross sections are moderate ranging from 20×10^{-20} to 2×10^{-20} m^2 for the range of impact energies considered here (1–50 kJ/mol). Second, the inefficient energy transfer in collisions of light H atoms with the heavy target atoms gives rise to a high specificity of the energy release. Only a fraction of no more than 5% of the available energy is channeled into relative translation of the HCl and Ar product. The remaining energy is found in the internal degrees of the HCl molecule which is vibrationally/rotationally extremly hot. The maxima of the distributions of internal energy correspond to $v=16$ and $J=20$ for the vibration and rotation, respectively. The extreme mass ratio also explains the angular distribution of the products which is essentially predetermined by the initial orientation of the ClAr dimer. In relatively rare cases of perpendicular collisions the H atom can be captured almost without direct interaction with the Ar atom which then leads to long-lived resonances with lifetimes of the HClAr complex in the order of picoseconds. These resonances are among the most interesting predictions of the calculations, and most experimental efforts should be directed towards seeing these manifestations of the "third body" effect.

Another important effect of a solvent is the "cage" effect. If a solvent shell isolates the reactants from each other the reactivity may be dramatically reduced. This phenomenon is studied here for the case of a Cl radical fully solvated by a shell of 12 Ar atoms. The minimum energy configuration of the $Cl(Ar)_{12}$ cluster is of icosahedral symmetry with the Cl atom in its center. In collisions of this aggregate with H atoms there are two completely different events. At low impact energies ($E_{coll}=0.1$ kJ/mol) we find a high cross section for physisorption of the incoming H atom in the van der Waals well formed by the cluster. After relaxation of its initial kinetic energy the H atom gets trapped on the surface of the doped Ar cluster. This trapping does not lead to HCl association. The lifetime of the H observed on the cluster is up to the nanosecond regime.

If the cluster is assumed to be initially "frozen" the effect of caging also remains prevalent for energies high enough ($E_{coll}=100$ kJ/mol) for cage penetration along certain directions. The H atoms are found to be scattered from the cluster without chemical reaction. To investigate the effect of cluster temperature on the reactivity a series of MD simulations of the $Cl(Ar)_{12}$ system is carried out. It is shown that the cluster is solid like at low temperatures. At a temperature of 40 K the amplitudes of the thermal motions of the atoms increase substantially but still there is no free mobility. At $T=45$ K the aggregate is finally found to be in a liquidlike state. In studying collisions with H atoms the role of temperature effects varies strongly with the impact energy. At a moderate energy of 10 kJ/mol we find a pronounced threshold behavior. Up to a temperature of 40 K the widening of the cage openings does not invoke any substantial reactivity. There is only a very low probability for cage penetrations with subsequent HCl recombination ($\sigma_R<0.5\times10^{-20}$ m^2). This changes drastically at $T=45$ K where due to the mobility of the atoms the Cl reagent is found to be exposed on the cluster surface which causes a sudden onset of large reactivity. This breakdown of the cage effect upon the solid–liquid transition of the solvent cluster tends to be washed out at higher impact energies. For $E_{coll}=100$ kJ/mol we find nonnegligible reactivity for temperatures where the cluster is still in the solidlike regime ($T\lesssim40$ K). Above the transition temperature there is no further increase of the reactive cross section. This is explained by a steric effect. The enhanced exposure of the Cl atom on one side of the cluster surface is compensated by shielding due to the 12 Ar atoms on the other side. It is emphasized that for not too high energies the use of association reactions to characterize cluster states as solids or liquids, and to observe the melting transition with temperature in cluster experiments is very promising.

Future work could be along two different directions. (1) The classical studies can be extended to also include larger

systems. Interesting topics are the following. What is the effect of more than one solvation shell? How is the association reaction affected if we consider the other reactant (or both) to be bound to a van der Waals cluster? (2) Another extremly important issue is the question of quantum effects in solvation dynamics. What is the role of zero-point energy of the cluster? What happens to the resonances found in the H+ClAr collisions? Can the cage effect of a complete solvation shell be reduced by tunneling? A natural approach to explore the quantum dynamics of the systems studied here could be quantum/classical TDSCF methods in which the dynamics of the H atom is treated fully quantum-mechanically while the motion of the heavy atoms is modeled by semiclassical techniques.[40,41] (3) Finally another interesting open issue is the role of nonadiabatic processes in this type of systems. The degenerate $2P$ state of the Cl atom certainly implies a possible role for coupling between different electronic states and more generally for the anisotropy of the Cl($2P$) interactions with other atoms. This aspect already received attention in recent studies of Cl and other open shell atoms in Ar matrices, and merits theoretical attention in the context of recombination.[23,74]

ACKNOWLEDGMENTS

The authors would like to thank J. Siebers (Max-Planck-Institut für Strömungsforschung, Göttingen, Germany) for his assistance with the MD simulations of the $Cl(Ar)_{12}$ system. One of us (B.S.) is recipient of a fellowship of the Minerva Society for Research, Munich, Germany. This society also supports the Fritz Haber Research Center. R.B.G. thanks the Alexander von Humboldt Stiftung for a Max Planck Research Award, which was used in part to support this work. Furthermore, hospitality of the Advanced Studies Institute, Hebrew University, Jerusalem, where part of the present work was carried out, is gratefully acknowledged.

[1] J. Troe, Annu. Rev. Phys. Chem. **29**, 223 (1978).
[2] J. Schroeder and J. Troe, Annu. Rev. Phys. Chem. **38**, 163 (1987).
[3] Gilbert and Smith, *Theory of Unimolecular and Recombination Reactions* (Blackwell, Oxford, 1990).
[4] R. Schinke, *Photodissociation Dynamics* (Cambridge, Cambridge, 1993).
[5] J. T. Hynes, Annu. Rev. Phys. Chem. **36**, 573 (1985).
[6] J. Franck and E. Rabinowitch, Trans. Faraday Soc. **30**, 120 (1934).
[7] B. Otto, J. Schroeder, and J. Troe, J. Chem. Phys. **81**, 202 (1984).
[8] D. E. Smith and C. B. Harris, J. Chem. Phys. **87**, 2709 (1987).
[9] A. L. Harris, J. K. Brown, and C. B. Harris, Annu. Rev. Phys. Chem. **39**, 341 (1988).
[10] K. Luther and J. Troe, Chem. Phys. Lett. **24**, 85 (1974).
[11] J. C. Dutoit, J. M. Zellweger, and H. van den Bergh, J. Chem. Phys. **78**, 1825 (1983).
[12] H. Hippler, V. Schuebert, and J. Troe, J. Chem. Phys. **81**, 3931 (1984).
[13] P. S. Dardi and S. J. Dahler, J. Chem. Phys. **93**, 242 (1990).
[14] J. N. Murrel, A. J. Stace, and R. Dammel, J. Chem. Soc. Faraday Trans. 2 **74**, 1532 (1978).
[15] D. J. Nesbitt and J. T. Hynes, J. Chem. Phys. **77**, 2130 (1982).
[16] V. E. Bondybey and C. Fletcher, J. Chem. Phys. **64**, 3615 (1976).
[17] V. E. Bondybey and L. E. Brus, Adv. Chem. Phys. **41**, 269 (1980).
[18] P. B. Beeken, E. A. Hanson, and G. W. Flynn, J. Chem. Phys. **78**, 5892 (1983).
[19] H. Kunz, J. G. McCaffrey, R. Schriever, and N. Schwentner, J. Chem. Phys. **94**, 1039 (1991).
[20] M. Chergui and N. Schwentner, Trends Chem. Phys. **2**, 89 (1992).
[21] (a) R. Alimi, R. B. Gerber, and V. A. Apkarian, J. Chem. Phys. **89**, 174 (1988); (b) **92**, 3551 (1990).
[22] R. Alimi, R. B. Gerber, J. G. McCaffrey, H. Kunz, and N. Schwentner, Phys. Rev. Lett. **69**, 856 (1992).
[23] I. H. Gersonde and H. Gabriel, J. Chem. Phys. **98**, 2094 (1993).
[24] G. G. Hammes, *Principles of Chemical Kinetics* (Academic, New York, 1978).
[25] *The Chemical Physics of Atomic and Molecular Clusters*, in *Proceedings of the Enrico Fermi Summer School*, edited by G. Scoles (Elsevier, Amsterdam, New York, 1990).
[26] *Atomic and Molecular Clusters*, edited by E. R. Bernstein (Elsevier, Amsterdam, 1990).
[27] M. Takayanagi and I. Hanazaki, Chem. Rev. **91**, 1193 (1991).
[28] X. J. Gu, D. J. Levandier, B. Zhang, G. Scoles, and D. Zhuang, J. Chem. Phys. **93**, 4898 (1990).
[29] S. Leutwyler and J. Bösiger, Chem. Rev. **90**, 489 (1990).
[30] K. L. Saenger, G. M. McClelland, and D. R. Herschbach, J. Phys. Chem. **85**, 3333 (1981).
[31] J. J. Valentini and J. B. Cross, J. Chem. Phys. **77**, 572 (1982).
[32] J.-M. Philippoz, R. Monot, and H. van den Bergh, J. Chem. Phys. **93**, 8676 (1990).
[33] D. Ray, N. E. Levinger, J. M. Papanikolas, and W. C. Lineberger, J. Chem. Phys. **91**, 6533 (1989).
[34] J. M. Papanikolas, J. R. Gord, N. E. Levinger, D. Ray, V. Vorsa, and W. C. Lineberger, J. Phys. Chem. **95**, 8028 (1991).
[35] S. Fei, X. Zheng, M. C. Heaven, and J. Tellinghuisen, J. Chem. Phys. **97**, 6057 (1992).
[36] I. NoorBatcha, L. M. Raff, and D. L. Thompson, J. Chem. Phys. **81**, 5658 (1984).
[37] J. A. Beswick, R. Monot, J.-M. Phillippoz, and H. van den Bergh, J. Chem. Phys. **86**, 3965 (1987).
[38] L. Perera and F. G. Amar, J. Chem. Phys. **90**, 7354 (1989); **93**, 4884 (1990).
[39] R. Alimi and R. B. Gerber, Phys. Rev. Lett. **64**, 1453 (1990).
[40] A. Garcia-Vela, R. B. Gerber, and J. J. Valentini, J. Chem. Phys. **97**, 3297 (1992).
[41] A. Garcia-Vela, R. B. Gerber, and D. G. Imre, J. Chem. Phys. **97**, 7242 (1992).
[42] A. Garcia-Vela and R. B. Gerber, J. Chem. Phys. **98**, 427 (1993).
[43] A. Garcia-Vela, R. B. Gerber, D. G. Imre, and J. J. Valentini, Chem. Phys. Lett. **202**, 473 (1993); Phys. Rev. Lett. **71**, 931 (1993).
[44] A. Garcia-Vela, R. B. Gerber, and U. Buck, J. Phys. Chem. (in press, 1994).
[45] J. Nieman and R. Naaman, J. Chem. Phys. **84**, 3825 (1986).
[46] J. Nieman, J. Shwartz, and R. Naaman, Z. Phys. D **1**, 231 (1986).
[47] J. P. Visticot, J. M. Mestdagh, C. Alcaraz, J. Cuvellier, and J. Berlande, J. Chem. Phys. **88**, 3081 (1988).
[48] A. Lallement, J. Cuvellier, J. M. Mestdagh, P. Meynardier, P. de Pujo, O. Sublemontier, J. P. Visticot, J. Berlande, and X. Biquard, Chem. Phys. Lett. **189**, 182 (1992).
[49] Y. Hurwitz, Y. Rudich, R. Naaman, and R. B. Gerber, J. Chem. Phys. **98**, 2941 (1993).
[50] X. Hu and W. L. Hase, J. Phys. Chem. **96**, 7535 (1992).
[51] X. Hu and C. C. Martens, J. Chem. Phys. **97**, 8805 (1992); **98**, 8551 (1993); **99**, 2654 (1993).
[52] R. A. Aziz and M. J. Slaman, Mol. Phys. **58**, 679 (1986).
[53] V. Aquilanti, D. Cappelletti, V. Lorent, E. Luzzatti, and F. Pirani, J. Phys. Chem. **97**, 2063 (1993).
[54] K. T. Tang and J. P. Toennies, Chem. Phys. **156**, 413 (1991).
[55] K. P. Hubert and G. Herzberg, *Molecular Spectra and Molecular Structure, Constants of Diatomic Molecules* (Van Nostrand, New York, 1979).
[56] R. A. Buckingham, Proc. R. Soc. A **168**, 264 (1938).
[57] J. M. Hutson, J. A. Beswick, and N. Halberstadt, J. Chem. Phys. **90**, 1337 (1989).
[58] A. R. Cooper and J. M. Hutson, J. Chem. Phys. **98**, 5337 (1993).
[59] (a) J. M. Hutson, J. Chem. Phys. **89**, 4550 (1988); (b) J. Phys. Chem. **96**, 4237 (1992).
[60] M. J. Elrod, J. G. Loeser, and R. J. Saykally, J. Chem. Phys. **98**, 5352 (1993).
[61] H. Goldstein, *Classical Mechanics* (Addison–Wesley, Reading, MA, 1950).
[62] R. N. Porter and L. M. Raff, in *Dynamics of Molecular Collisions*, edited by W. H. Miller (Plenum, New York, 1976), Part B, p. 1.

[63] C. W. Gear, *Numerical Initial Value Problems in Ordinary Differential Equations* (Clarendon, Oxford, 1971).
[64] R. D. Levine and R. B. Bernstein, *Molecular Reaction Dynamics and Chemical Reactivity* (Oxford University, Oxford, 1987).
[65] P. J. Kuntz, in *Dynamics of Molecular Collisions*, edited by W. H. Miller (Plenum, New York, 1976), Part B, p. 53.
[66] A. L. Mackay, Acta Crystallogr. **15**, 916 (1962).
[67] M. R. Hoare and P. Pal, Adv. Phys. **24**, 645 (1975).
[68] J. Farges, M. F. de Feraudy, B. Raoult, and G. Torchet, J. Chem. Phys. **78**, 5067 (1983); **84**, 3491 (1986).
[69] J. Siebers (private communication, 1993).
[70] G. Del Mistro and A. J. Stace, Chem. Phys. Lett. **196**, 67 (1992).
[71] F. A. Lindemann, Z. Phys. **11**, 609 (1911).
[72] C. L. Briant and J. J. Burton, J. Chem. Phys. **63**, 2045 (1975).
[73] J. Jellinek, T. L. Beck, and R. S. Berry, J. Chem. Phys. **84**, 2783 (1986).
[74] A. I. Krylov and R. B. Gerber, J. Chem. Phys. **100**, 4242 (1994).